communications physics

A Nature Portfolio journal

Article

https://doi.org/10.1038/s42005-025-02413-6

Social polarization promoted by sparse higher-order interactions

Hugo Pérez-Martínez [1,2], Santiago Lamata-Otín [1,2], Federico Malizia [3], Luis Mario Floría[1,2], Jesús Gómez-Gardeñes [1,2,4,6] ✉ & David Soriano-Paños [1,5,6] ✉

Many social interactions are group-based, yet their role in social polarization remains largely unexplored. To bridge this gap here we introduce a higher-order framework that takes into account both group interactions and homophily. We find that group interactions can strongly enhance polarization in sparse systems by limiting agents' exposure to dissenting views. Conversely, they can suppress polarization in fully connected societies, an effect that intensifies as the group size increases. Our results highlight that polarization depends not only on the homophily strength but also on the structure and microscopic arrangement of group interactions.

Understanding how human interactions in large-scale societies generate consensus, cooperation, political identities, or persistent divisions remains a central challenge in modern social science[1,2]. During the last two decades, the statistical physics community has devoted substantial effort to explaining how macroscopic collective behavior can emerge from simple microscopic interaction rules[3,4]. Among these phenomena, the emergence of *polarization* has become a paradigmatic problem, whose relevance continues to grow due to the increasing availability of data from digital media[5–7].

Many mathematical models of opinion dynamics based on consensus have successfully captured the processes of consensus formation, since the seminal work by DeGroot[8] to the traditional bounded-confidence models like the Deffuant-Weisbuch model[9] and the Hegselmann-Krause model[10]. Moreover, opinion dissensus in the form of fragmentation has also been widely reported in the latter models due to the bounded-confidence mechanism, as well as in other works that include distancing[11,12] or other forms of antagonistic interactions[13–15].

However, the typical equilibrium states of these models fail to reproduce the bimodal opinion distributions usually observed in empirical data on polarized issues[16,17], which tend to show rich opinion landscapes in which people place themselves in some intermediate positions distributed along the whole possible range, rather than in a limited set of choices populated by a group of completely agreeing agents. Moreover, the phenomenon of distancing is still widely contested in the literature, as it warrants further analysis of the conditions needed for its occurrence[18–20]. Instead, other models based on the phenomenon of group polarization[21,22] have been proven to capture the onset of polarization successfully while retaining a rich opinion landscape[23–26]. Group polarization is one of the most documented phenomena that guide opinion formation processes, and it considers that a group of interacting individuals does not converge to the average opinion of the group, but rather becomes more radicalized in the original average opinion's direction[27]. For example, a jury in which members are, on average, relatively convinced of the guilt of the defendant will turn out to be strongly convinced after deliberation[28]. The model we present below follows this approach to study the emergence of opinion polarization.

All the aforementioned works, as well as other socio-physical models[29–35], represent the backbone of human interactions as complex networks[36,37]. Yet, in real-world settings, opinions are rarely shaped through isolated dyadic interactions, since they are formed, reinforced, or challenged within actual groups of more than two individuals. From informal discussions to deliberative assemblies, those higher-order (i.e., group-based) interactions[38–43] represent the native environment of opinion formation. This is made specially clear on the phenomenon of group polarization where, as its name implies, most experiments are performed on groups[44–46]. Although recent studies have incorporated higher-order influence into consensus and fragmentation dynamics, either through diffusion-like processes[47–52] or by generalizing bounded confidence models[53–55], the role of group structure in driving group polarization remains largely unexplored.

In this article, we aim to tackle this problem by introducing a dynamical framework for opinion formation that extends the empirically grounded mechanism of group polarization to explicitly incorporate group interactions, encoded via higher-order networks. We find that group interactions promote radical consensus only when they dominate the dynamics. In contrast, when pairwise interactions prevail, sparse higher-order interactions enhance polarization by reinforcing local agreement within groups. Furthermore, we show through analytical

[1]GOTHAM lab, Institute for Biocomputation and Physics of Complex Systems (BIFI), University of Zaragoza, Zaragoza, Spain. [2]Department of Condensed Matter Physics, University of Zaragoza, Zaragoza, Spain. [3]Department of Network and Data Science, Central European University, Vienna, Austria. [4]Center for Computational Social Science, University of Kobe, Kobe, Japan. [5]Departament d'Enginyería Informàtica i Matemàtiques, Universitat Rovira i Virgili, Tarragona, Spain. [6]These authors jointly supervised this work: Jesús Gómez-Gardeñes, David Soriano-Paños. ✉e-mail: gardenes@unizar.es; sorianopanos@gmail.com

results that the impact of group interactions intensifies with increasing group size. Our findings show that polarization depends not only on the homophily strength but also on the structural arrangement of social interactions, providing new insights into how group dynamics shape collective opinion formation.

Results

Opinion dynamics with higher-order interactions

We model the structure of social interactions by means of a hypergraph $\mathcal{H}$ formulation. This type of structure is defined as a pair $\mathcal{H} = (\mathcal{N}, \mathcal{E})$, where $\mathcal{N}$ is the set of N nodes (here the agents), and $\mathcal{E}$ is a collection of subsets of $\mathcal{N}$ called *hyperedges*. Each hyperedge $\gamma \in \mathcal{E}$ represents a group of agents that interact simultaneously. The *order* of a hyperedge is given by the number of agents it connects minus one; that is, a hyperedge γ of size $m+1$ is said to be of order m. This way, 1-hyperedges correspond to pairwise interactions, 2-hyperedges to triplets, and so on, up to the maximum order of interaction M. The set $\Gamma_i^{(m)}$ is the collection of all the hyperedges of order m to which node i belongs and its cardinality corresponds to the generalized degree of order m of node i, defined as $k_i^{(m)}$.

To investigate how higher-order interactions shape collective opinion dynamics, we consider a framework in which each agent i holds a continuous opinion variable $x_i \in \mathbb{R}$, whose sign $\sigma(x_i) \equiv \sigma_i$ represents the qualitative position of the agent (in favor or against). In its turn, the module $|x_i|$ captures the strength of her belief.

The opinion of each agent, i.e., the value of x_i, evolves in time due to their associated group-based interactions according to:

$$\dot{x}_i = -x_i(t) + \sum_{m=1}^{M} \lambda^{(m)} \left[\sum_{\gamma \in \Gamma_i^{(m)}} w_i^{\gamma}(t) \tanh\left(\sum_{\substack{j \in \gamma \\ j \neq i}} \frac{x_j(t)}{m} \right) \right]. \quad (1)$$

This set of coupled differential equations generalizes the model introduced in ref. 25 to include higher-order interactions. The first term describes memory loss, while the second term pulls agents in the direction of their contacts' opinions (specially those more radical ones). In the case of groups, they influence agents' opinions in the direction of the average position of the group excluding the focal agent. This reproduces the effect of group polarization, as a group mildly in favor or against a given issue will become more radical after interacting. Additionally, $\lambda^{(m)}$ represents the *social interaction strength* of hyperedges of order m over the agent's opinion, and w_i^{γ} represents the importance that the agent gives to hyperedge γ, and thus, the influence that the group exerts over the agent (see Fig. 1a for a schematic representation of the model). Each weight w_i^{γ} evolves in time since it depends on the opinions of the agents in hyperedge γ, being its precise form:

$$w_i^{\gamma} = \frac{\left(\sum_{j \in \gamma} |x_i - x_j| + \epsilon^{(m)}\right)^{-\beta}}{\sum_{\xi \in \Gamma_i^{(m)}} \left(\sum_{l \in \xi} |x_i - x_l| + \epsilon^{(m)}\right)^{-\beta}}, \quad (2)$$

where β is the homophily parameter, and $\epsilon^{(m)}$ is a small regularizing constant (set to $\epsilon^{(m)} = 0.002\lambda^{(m)}$) introduced to avoid divergences for nearly identical opinions. This definition ensures that groups with agents having opinions more aligned with that of agent i exert a stronger influence, thus capturing the effect of homophily at the level of hyperedges.

Altogether, the dynamics of the system gives rise to three qualitatively distinct collective states: a *neutral consensus*, where all agents converge to a moderate opinion; a *radical consensus*, characterized by unanimous but extreme views; and a *polarized state*, in which the population splits into opposing opinion blocks. Figure 1b displays representative opinion trajectories for $M = 2$, corresponding to the three collective states described above. The dynamics were simulated on a Random Simplicial Complex (RSC) consisting of $N = 1899$ nodes, with average degree $\langle k^{(1)} \rangle = 10$ for pairwise interactions and a sparser higher-order connectivity characterized by $\langle k^{(2)} \rangle = 3$. Simplicial complexes fulfill the downward closure condition: 2-hyperedges include all possible 1 − hyperedges that can be formed between their nodes. Moreover, we impose that all agents belong to at least one group interaction, and that the higher-order network is connected in both interaction orders. Further information on how these configurations are built can be found in the Methods section and in ref. 41.

Our model yields polarization either as wide opinion distributions, with agents holding milder views, or as strongly radicalized populations, displaying two major opposed groups with extreme opposite opinions. These latter states, represented in the fourth trajectory, can resemble typical fragmented states obtained in bounded confidence models like the Hegselmann-Krause model[10] or the Deffuant-Weisbuch model[9]. However, we still consider such states to be polarized rather than fragmented because (i) there is is still communication and opinion share between agents regardless of the clusters they belong to, as weights are small but never zero, (ii) there is a smooth transition by varying β from wide, bimodal distributions shown in the third trajectory (that can be clearly identified with polarization) to the sharp ones shown in the fourth, indicating a clear relationship between them, and (iii) even for higher values of β, the clusters placed in the two most extreme opinions are always overwhelmingly dominant, which can be arguably seen as a form of extreme polarization.

Conversely, as derived in the Methods section, reaching neutral consensus is only possible when the total interaction strength remains below the

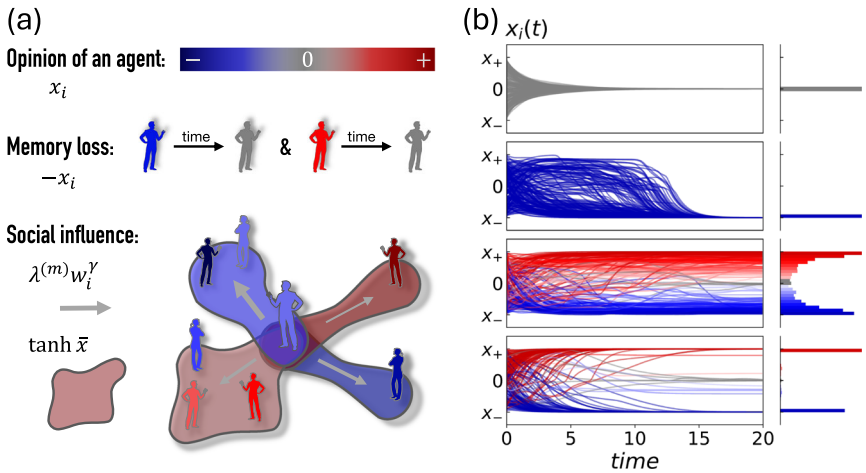

Fig. 1 | Opinion dynamics with higher-order interactions. a Schematic representation of the model: the memory loss term pulls agents toward a neutral opinion, while the social influence term pulls agents in the direction of the opinions of their acquaintances. **b** Temporal evolutions of agents in the representative configurations and resulting opinion distributions. From top to bottom: neutral consensus ($\lambda^{(1)} = \lambda^{(2)} = 0.4$, $\beta = 0.7$), radicalization ($\lambda^{(1)} = \lambda^{(2)} = 10$, $\beta = 0.2$) and polarization, which can appear as wide opinion distributions ($\lambda^{(1)} = \lambda^{(2)} = 10$, $\beta = 0.4$) or as sharp polarization ($\lambda^{(1)} = \lambda^{(2)} = 10$, $\beta = 1.5$). All results are for a Random Simplicial Complex (RSC) of $N = 1899$ nodes, $\langle k^{(1)} \rangle = 10$ and $\langle k^{(2)} \rangle = 3$. Initial opinions are randomly chosen on the interval $[x_-, x_+] = [-20, 20]$ (except for the top panel, where $[x_-, x_+] = [-1, 1]$), and the final opinion of the agents determines the color code.

critical threshold,

$$\sum_{m=1}^{M} \lambda^{(m)} < 1\,, \tag{3}$$

so that the first (dissipative) term in Eq. (1) prevails and most of opinions concentrate around 0. Remarkably, despite the non-linear nature of the dynamics, higher-order interactions contribute linearly across orders, with each $\lambda^{(m)}$ playing a direct role in driving the system away from neutral consensus. If the combined strength does not satisfy Eq. (3), the system reaches polarized or radicalized configurations.

Sparse higher-order interactions promote polarization

Now we move beyond the neutral consensus scenario by investigating how the interplay between social interaction strength, group structure, and homophily governs the emergence of either polarization or radicalization. To this aim, we fix $M = 2$, a large total interaction strength, $\lambda^{(1)} + \lambda^{(2)} = 20$, and we define $\delta = \lambda^{(2)}/20$ to interpolate between purely pairwise ($\delta = 0$) and purely higher-order ($\delta = 1$) regimes. As a proxy for polarization, we measure the fraction of configurations in which the standard deviation of opinions exceeds the absolute value of the mean, i.e., $\sigma > |\bar{x}|$, where $\bar{x} = \sum_i x_i/N$ and $\sigma^2 = \sum_i (x_i - \bar{x})^2/N$.

Figure 2a shows the fraction of polarized configurations as a function of the higher-order weight δ and the homophily parameter β. For each parameter set, we perform 100 independent runs with uniformly distributed random initial opinions (see Methods for the numerical integration details). For $\delta = 0$ (pairwise interactions only), we observe a clear transition from mixed states (polarization and radical consensus) to fully polarized configurations at a critical value $\beta_c = 1$, a threshold that can be derived analitically. Interestingly, polarization is already prominent around $\beta \simeq 0.4$, a regime in which the low value of homophily is compensated by the limited neighborhood of the agents imposed by the underlying structure, which facilitates the emergence of opposing radical clusters. These findings are already reported and explored in ref. 25, which focuses on strict pairwise interactions. Regarding the inclusion of higher-order interactions, as δ increases the system becomes increasingly susceptible to polarization for high values of β, noticeable from the decrease in the value of β_c required for its onset that promotes the emergence of polarization well into $\beta < 1$. However, this behavior is softened for $\delta \gtrsim 0.2$: the threshold β for full polarization starts to rise, and for $\delta \gtrsim 0.5$ the system recovers the usual transition at $\beta_c \simeq 1$. Regarding intermediate values of β, polarization fades around $\delta \simeq 0.5$ when both pairwise and higher-order interactions are present equally, but is recovered when higher-order interactions dominate ($\delta \to 1$).

These results uncover a non-trivial role of higher-order interactions in shaping collective dynamics. When pairwise interactions dominate, even weak group influence amplifies polarization, whereas dominant group interactions tend to restore the behavior of purely pairwise systems. However, despite the similarities in polarization fractions found between both regimes, there are substantial quantitative differences in the subjacent dynamics. To illustrate them, Fig. 2b, c show the equilibrium opinion distribution of the polarized configurations at fixed homophily $\beta = 0.4$, comparing the pairwise limit ($\delta \to 0$) to the regime dominated by higher-order interactions ($\delta \to 1$). In the latter case, opinions concentrate sharply around the extremal values, reflecting a population split into strongly radicalized cohesive groups holding opposite-sign views.

We start by analyzing first the system's behavior for intermediate values of β. To understand the effect of higher-order interactions, we must first briefly explain the purely pairwise scenario ($\delta = 0$), already covered in ref. 25 (we refer the reader to Supplementary Note 1 for a more detailed description of the original model and its basic results). The existence of polarization for $\beta < 1$ in sparse networks can be explained by considering that lower degrees facilitate the presence of homogeneous environments: it is less probable to find at least one cross-cutting interaction, thus encouraging polarization by radicalizing agents in opposite directions. In denser structures, cross-cutting interactions are enough to depolarize the system. (in ref. 25 it is proven that, in a completely dense dyadic graph, polarization is only stable if $\beta > 1$). Moreover, there is a clear effect with β, such that intermediate values of the homophily parameter around $\beta \simeq 0.4$ greatly promote polarization compared to higher values, around $\beta \lesssim 1$, even though homophily is stronger in the latter case. To understand this phenomenon, we note that agents are more likely to hold intermediate positions the lower the value of β, which stabilizes opinion distributions by providing screening to agents more exposed to cross-cutting interactions.

Since groups influence agents in a similar way as individual neighbors, the same reasoning applies when only group interactions are present ($\delta = 1$): if most groups are homogeneous and few are heterogeneous, agents radicalize in opposite directions, leading to polarization. As can be seen in

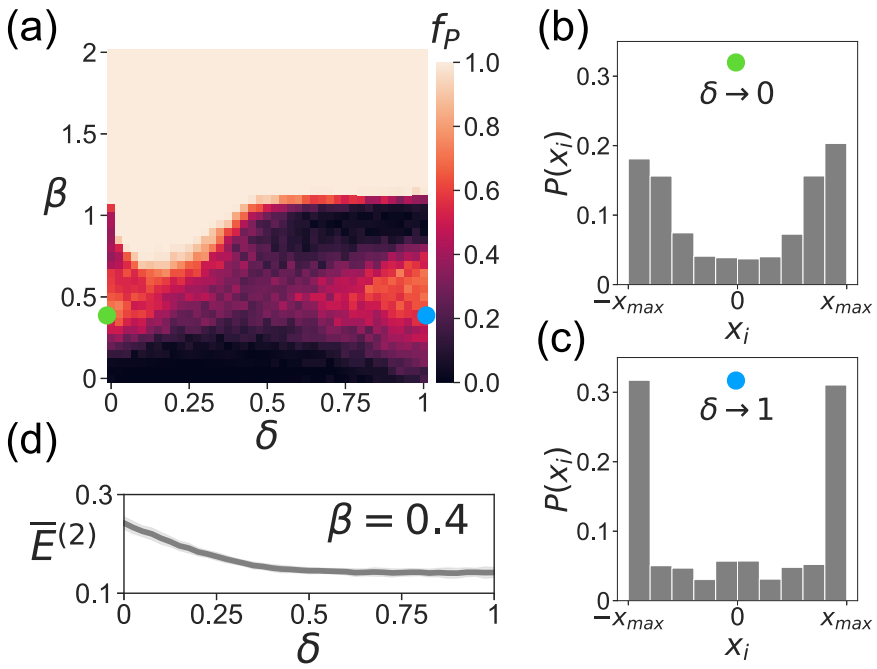

Fig. 2 | Sparse higher-order interactions promote polarization. a Fraction of polarized configurations f_P obtained from 100 independent realizations for each combination of parameters (δ, β) (color code). **b**, **c** Average opinion histograms obtained from 100 polarized configurations for $\delta = 0$ (green dot in (**a**)) and $\delta = 1$ (blue dot in (**b**)) given $\beta = 0.4$. **d** Average exposure $\bar{E}^{(2)}$ as a function of δ for $\beta = 0.4$, obtained from 100 polarized configurations for each parameter combination. Shadowed region corresponds to the standard deviation. All results are for an RSC of $N = 1899$ nodes, $\langle k^{(1)} \rangle = 10$ and $\langle k^{(2)} \rangle = 3$. Initial opinions are randomly chosen on the interval $[-20, 20]$. Each realization was run for 10,000 steps, corresponding to 1000 time units.

Fig. 2c, most agents hold extremely radical positions, which suggests that cross-cutting interactions are indeed largely absent for a sizeable fraction of them. To measure the extent of an agent's isolation from dissent through group interactions, we define the *exposure* of an agent i to cross-cutting relationships within its higher-order neighborhood as:

$$E_i^{(2)} = \frac{1}{|\Gamma_i^{(2)}|} \sum_{\gamma \in \Gamma_i^{(2)}} (1 - \delta_{\sigma_i,\sigma_\gamma}) . \quad (4)$$

In this expression, $\Gamma_i^{(2)}$ is the set of 2-hyperedges involving agent i, σ_i represents the sign of agent's i opinion, and σ_γ denotes the sign of the average opinion within group γ, excluding i. $\delta_{\sigma_i,\sigma_\gamma}$ denotes the Kronecker delta of the opinions signs, so that $\delta_{\sigma_i,\sigma_\gamma} = 1$ if both have the same sign, and 0 otherwise. The quantity $E_i^{(2)}$ therefore measures the fraction of cross-cutting higher-order interactions for a given agent. Note that a group is not classified as cross-cutting if the average group opinion aligns with σ_i, even when one member disagrees; this occurs when agreeing agents are sufficiently radicalized to compensate the opinions of disagreeing ones.

Figure 2d shows the average exposure $\bar{E}^{(2)} = N^{-1}\sum_{i=1}^{N} E_i^{(2)}$ as a function of δ for fixed $\beta = 0.4$, computed from 100 polarized configurations for each parameter combination. In the $\delta \to 0$ regime, in which pairwise interactions prevail, exposure to cross-cutting group interactions is relatively high, but their weakness in comparison to pairwise interactions makes equilibrium opinion distributions largely impervious to them, thus mostly maintaining polarization. For increasing values of δ, the incremental strength of group interactions reflects in the growing internal homogeneity of 2-hyperedges, decreasing exposure. However, greater group influence also amplifies agents' reach, whose dynamics become dominated both by pairwise and higher-order interactions at the same time, thus diminishing the effective sparsity of the network and proving to be detrimental for polarization. This effect is further amplified when relaxing the closure condition, as the set of neighbors through pairwise and group interactions are no longer completely overlapping, increasing the agent's reach inside the network (see Supplementary Fig. 2 in Supplementary Note 2). Finally, when $\delta \to 1$, group interactions dominate completely, making pairwise interactions irrelevant and facilitating the emergence of polarized states again, associated with sharper opinion distributions because of the very limited exposure to cross-cutting interactions measured by the exposure (see Fig. 2c).

Apart from the aforementioned results, weak higher-order interactions strongly promote polarization for $\beta \lesssim 1$, although this effect vanishes when they become dominant. Therefore, it emerges when groups interactions could be considered as a perturbation with respect to pairwise coupling, slightly displacing the equilibrium opinions of the agents and creating new positions where they can get trapped, but without the strength to overturn the sign of an agent's opinion regardless of her exposure to cross-cutting interactions. This effect can be understood again by the limited exposure to cross-cutting groups product of the higher-order network sparsity: as many agents have low higher-order degrees, they belong only to either homogeneous or heterogeneous groups that displace their equilibrium opinions slightly to one side or the other. In the former case, they act as a net polarizing force, as they pull opposite agents farther apart. In the latter, they displace the agents toward milder views, contributing to wider opinion distributions while lacking the force to overturning agents' opinions completely, also reinforcing polarization. For increasing higher-order strength ($\delta \simeq 0.5$), this effect disappears again for the same reason explained for the scenario around $\beta \simeq 0.4$: both interaction orders compete in equal manner, increasing the effective reach of the agents that get exposed to a higher share of cross-cutting interactions with the potential of turning them, and ultimately negating the beneficial effect of sparse networks in polarization. Therefore, this effect is highly contingent on the network structure, as we will explore in the next section.

Dense higher-order interactions suppress polarization

Having established that sparse higher-order interactions can promote polarization, we now investigate the role of increasing the net structural prominence of group interactions. To do so, we consider three different higher-order networks with $\langle k^{(1)} \rangle = 10$ and different connectivities of group interactions $\langle k^{(2)} \rangle \in \{3, 7, 15\}$. Additionally, as the downward closure condition cannot be fulfilled for higher degrees, instead of simplicial complexes we construct hypergraphs that exhibit the maximum possible inter-order hyperedge overlap[56] for each chosen pair of macroscopic connectivities ($\langle k^{(1)} \rangle$, $\langle k^{(2)} \rangle$) (see Methods for the crafting details).

In Fig. 3a, we show the fraction of polarized configurations as a function of δ and the homophily parameter β, for the three different connectivities. The results reveal that polarization is strongly suppressed as agents' reach increases (larger connectivity values), confirming the structural origin of the phenomena reported in the previous section. In particular, polarized states at intermediate values of β (around $\beta \approx 0.5$) disappear in the regime of dominating higher-order interactions, confirming that they were caused by the network sparsity. Moreover, the size of the polarization bump found under weak higher-order influence also shrinks as the $2-$hyperedges degree increases.

To showcase the effect of higher-order degree in polarization, we show in Fig. 3b the distribution of exposures in equilibrium polarized opinion distributions, computed for a parameter combination inside the polarization bump in the three cases contemplated in panel a. For low degrees, it is clear that some agents retain cross-cutting interactions ($E_i^{(2)} \neq 0$), while others are embedded in completely homogeneous environments ($E_i^{(2)} = 0$).

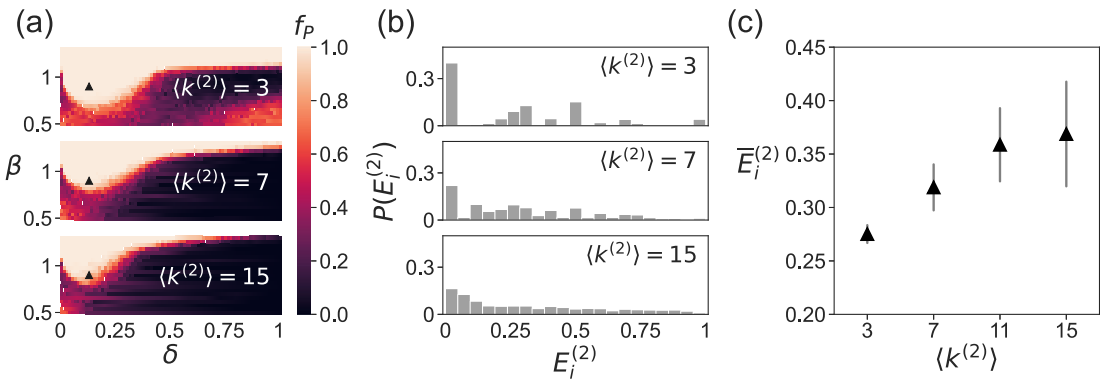

Fig. 3 | Dense group interactions suppress polarization. a Fraction of polarized configurations obtained from 100 independent realizations for each combination of parameters (δ, β) (color code), for structures with different $\langle k^{(2)} \rangle$, $\langle k^{(1)} \rangle = 10$, and maximum inter-order hyperedge overlap. **b** Distribution of exposures $E_i^{(2)}$ for 100 polarized configurations generated with parameters $\delta = 0.125$ and $\beta = 0.9$ and different $\langle k^{(2)} \rangle$ (pinpointed with a black triangle in **a**). **c** Average exposure $\bar{E}^{(2)}$ as a function of $\langle k^{(2)} \rangle$, for $\delta = 0.125$ and $\beta = 0.9$ (points highlighted on **a**), obtained from 100 independent realizations for each point. Bars represent the standard deviation. Networks are comprised of $N = 2000$ nodes, except the graph of $\langle k^{(2)} \rangle = 3$, which has $N = 1899$. Each realization was run for 10000 steps, corresponding to 1000 time units.

However, as $\langle k^{(2)} \rangle$ increases, the neighborhoods of agents become more diverse, and it is increasingly difficult to avoid cross-cutting interactions. This tendency is clearly captured by measuring the average exposure $\bar{E}^{(2)}$ as a function of $\langle k^{(2)} \rangle$, which we represent in Fig. 3c: it becomes clear that higher degrees entail greater exposures, negating the occurrence of homogeneous environments and making polarization more difficult.

Finally, we remark that heterogeneous groups can sustain intermediate opinions closer to the focal agent, which exert stronger influence and thus enhance the depolarizing effect compared to simple pairwise interactions, where cross-cutting ties are more distant and extreme. This effect is reflected in the gradual increase in the value of β_c with δ for strong higher-order interactions, i.e. for $\delta > 0.5$. The following section provides a plausible explanation for the detrimental effect of group interactions in polarization, derived by their effect on the polarization threshold β_c.

Analytical derivation of the polarization threshold

To quantify the shift on the polarization threshold when higher-order interactions are dense and dominant, we analyze the stability of fully polarized states in fully connected hypergraphs, where each agent participates in all possible m-hyperedges up to order M. We consider a configuration in which N_+ agents hold a positive opinion x_+ and $N_- = N - N_+$ hold a negative opinion x_-. Through a linear stability analysis (detailed in Methods and Supplementary Note 3), we reveal that such polarized states are stable provided the homophily parameter β exceeds a critical threshold β_c, determined implicitly by

$$\beta_c \sum_{m=1}^{M} \lambda^{(m)} f(m, \lambda^{(m)}, \beta_c) = 1, \tag{5}$$

where $f(m, \lambda^{(m)}, \beta_c)$ is detailed in the Methods section.

In Fig. 4a we show the behavior of β_c as a function of M for two scenarios. Firstly, we consider the case of fully connected simplicial complexes with interactions up to order M (with $\lambda^{(m)} = 20/M \,\forall\, m$), and secondly, fully connected M-uniform hypergraphs only containing all possible order-M interactions, with $\lambda^{(M)} = 20$. In both cases, β_c increases with M, indicating that polarization becomes progressively harder to sustain with increasing group size. Our analytical predictions are in excellent agreement with numerical integration of the full dynamics for $N = 100$ agents.

As hinted before, the mechanism behind this effect lies on the existence of cross-cutting hyperedges that also include agreeing agents, making the group more influential while still acting as a depolarizing force, thus requiring higher values of homophily, β, to compensate. As we saw before, in the case of networked populations these heterogeneous groups could be absent for a non-negligible set of agents, but in the case of fully connected hypergraphs or order m, for a given agent holding opinion x_+, there are

$$n_m(b) = \binom{N_+}{m-b}\binom{N_-}{b} \tag{6}$$

such groups with b neighbors with opposite opinion (x_-), and $m - b$ with the same opinion (x_+).

In Fig. 4b we represent $n_m(b)$ as a function of the average opinion of these groups based on the order m. For pairwise interactions ($m = 1$), we find that the neighboring agents can exhibit only purely positive/negative opinions. However, as group size increases, a rich repertoire of mixed compositions emerges. In larger groups, agents often share cross-cutting m-hyperedges with some like-minded individuals, rather than being completely isolated. For example, a positive-opinion node in a 3-hyperedge might encounter two negative agents and one other positive agent. While the group average remains negative, it is much closer to zero than if all three other members held negative views. In other words, larger groups that produce more moderate collective opinions include agreeing neighbors. As a result, they are more effective at pulling agents toward the center and the opposite view, resulting in radicalized societies.

Discussion

In this article, we have introduced a dynamical framework for opinion formation considering the group polarization phenomenon that explicitly incorporates homophily and group interactions through higher-order networks. Our results reveal a fundamental asymmetry in how group structure shapes collective opinion dynamics. While sparse group interactions amplify polarization, with agents encountering limited dissenting views, dense group interactions suppress polarization by exposing agents to more moderate collective opinions through compositional diversity. Moreover, the larger the group size, the more prominent those effects are.

Unlike previous models, in which only pairwise interactions were considered, here the existence of higher-order interactions provides a mechanism for the emergence and loss of polarization that can be understood through the exposure of agents to opposite opinions through groups. In this respect, networked populations with sparse higher-order interactions are prone to the presence of homogeneous groups in which everyone agrees without any dissent, thus becoming a net polarizing force.

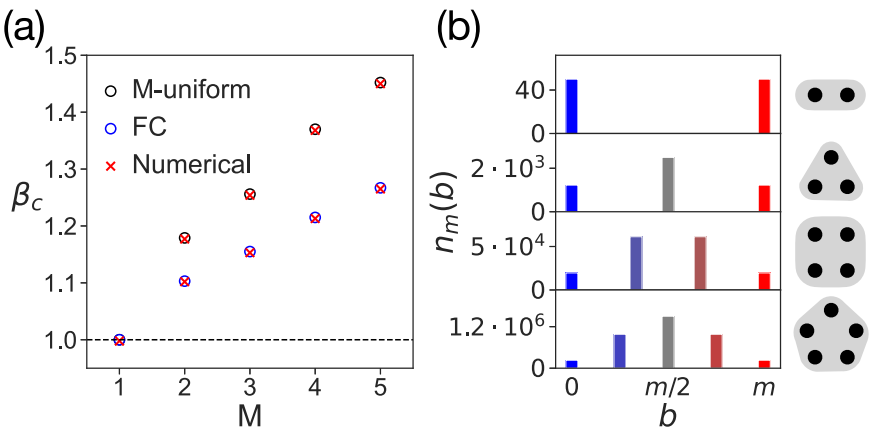

Fig. 4 | Analytical derivation of the polarization threshold. a Stability thresholds β_c for a polarized configuration computed from Eq. (18) considering M-uniform hypergraphs (black circles) and fully-connected hypergraphs up to order M (blue circles), as a function of the highest order present in the network. Results are shown together with the numerical values obtained by running the system of N equations for validation purposes (red crosses). Throughout the figure, we consider networks comprised of $N = 100$ agents. **b** Number of groups $n_m(b)$ to which an agent is exposed comprised by b neighbors of opinion x_- and $m - b$ neighbors of opinion x_+, as a function of b. The color code reflects the proportion of the groups, going from blue corresponding to groups with all agents with positive opinions to red where all agents hold negative opinions. Multiple orders of interaction are shown, from $m = 1$ (top) to $m = 4$ (bottom). An schematic representation of the interactions of order m is presented alongside its corresponding histogram, where the shadowed region depicts the hyperedge connecting the $m + 1$ nodes (represented by black dots).

However, when group interactions are more prominent in connecting the network, either because of being dense or because having low hyperedge overlap[56,57], cross-cutting groups become increasingly probable while usually containing agreeing individuals at the same time. This increases their influence and drives their constituents towards the majority, encouraging agreement.

Indeed, our results are consistent with recent findings pinpointing that higher-order interactions favor consensus, as being exposed to intermediate opinions greatly favors agreement within a group[49,53,54]. However, as we have discussed, this effect is contingent upon certain network characteristics, that cannot be overlooked. Our framework thus provides a foundation for the development of more advanced frameworks that capture key structural features of higher-order networks, such as their temporal evolution[58–60], and how they shape the emergence of polarization in real-world systems.

Methods

Crafting of higher-order structures

Random Simplicial Complex (RSC). In our manuscript, we considered Random Simplicial Complexes (RSCs) of order $M = 2$ generated following the model introduced by Iacopini et al.[41]. Given a set of N nodes, each pair of nodes (i, j) is connected with probability $p^{(1)}$, resulting in an Erdős-Rényi graph with average 1-degree $\langle k^{(1)}\rangle = (N-1)p^{(1)}$. Moreover, each triplet (i, j, k) is filled with a 2-simplex with probability $p^{(2)}$, regardless of whether its edges are already present. The average 2-degree is then $\langle k^{(2)}\rangle = \frac{(N-1)(N-2)}{2}p^{(2)}$. Each 2-simplex contributes, on average, $2(1-p^{(1)})$ additional links to the 1-degree of its nodes, depending on whether the corresponding edges (1-faces) were already present. As a result, the expected total 1-degree becomes: $\langle k^{(1)}\rangle_{\text{total}} \approx (N-1)p^{(1)} + 2\langle k^{(2)}\rangle(1-p^{(1)})$. As a consequence, to craft a RSC with target values of $\langle k^{(1)}\rangle$ and $\langle k^{(2)}\rangle$, the connection probabilities to be chosen are:

$$p^{(1)} = \frac{\langle k^{(1)}\rangle - 2\langle k^{(2)}\rangle}{(N-1) - 2\langle k^{(2)}\rangle}, \tag{7}$$

$$p^{(2)} = \frac{2\langle k^{(2)}\rangle}{(N-1)(N-2)}. \tag{8}$$

Note that, in order to ensure the connectedness of the structure, we remove the nodes which are disconnected. This is the reason why the structure utilized in Figs. 1 and 2 has $N = 1899$ instead of the original $N = 2000$.

Hypergraphs with maximum inter-order hyperedge overlap. If $2\langle k^{(2)}\rangle > \langle k^{(1)}\rangle$, Eq. (7) yields negative values, as there are no enough $1-$ hyperedges to fill all the faces of the $2-$ hyperedges. Therefore, in these situations, we craft hypergraphs that maintain the downward closure to the best extent, i.e., with maximum inter-order hyperedge overlap[56]. In order to do so, we first create the set of $2-$ hyperedges according to Eq. (8), and afterwards, we sample as $1-$ hyperedges a fraction of the faces of the $2-$ hyperedges, according to the probability

$$\bar{p}^{(1)} = \frac{k^{(1)}}{2k^{(2)}}. \tag{9}$$

Analytical derivation of the transition to consensus

Neutral consensus corresponds to the fixed point $x_i = 0\ \forall i \in \mathcal{N}$. To determine its stability we perform a mean field analysis from Eqs. (1)–(2) by assuming that all agents hold similar opinions, i.e., $x_j \approx x$. We therefore approximate each group average as $\sum_{j\in\gamma} x_j/m \approx x$, and the weights become uniform across hyperedges. This reduces Eq. (1) to

$$\dot{x} = -x + \sum_{m=1}^{M} \lambda^{(m)} \tanh(x). \tag{10}$$

In the stationary state, where $\dot{x} = 0$, Eq. (10) yields a scalar fixed-point equation:

$$x = \sum_{m=1}^{M} \lambda^{(m)} \tanh(x). \tag{11}$$

Since $\tanh(0) = 0$, the solution $x = 0$ always exists. To assess its stability, we linearize Eq. (10) around $x = 0$, using $\tanh(x) \approx x$, yielding

$$\dot{\varepsilon} \approx -\varepsilon + \left(\sum_{m=1}^{M} \lambda^{(m)}\right)\varepsilon = \varepsilon\left(-1 + \sum_{m=1}^{M} \lambda^{(m)}\right). \tag{12}$$

Hence, $x = 0$ is stable if

$$\sum_{m=1}^{M} \lambda^{(m)} < 1, \tag{13}$$

and unstable otherwise. This condition defines the critical surface in parameter space where the neutral consensus loses stability and non-zero solutions (corresponding to polarization or radical consensus) emerge.

Numerical integration details

The system of N coupled differential equations is integrated using an explicit fourth-order Runge-Kutta method with a time step $dt = 0.1$.

Stability analysis of a polarized configuration

We perform a linear stability analysis of a polarized configuration, in which N_+ agents take a positive opinion x_+ and $N_- = N - N_+$ a negative opinion x_-. In Supplementary Note 3 we derive that, in the equilibrium, both opinions fulfill the system of equations:

$$x_+ = \sum_{m=1}^{M} \lambda^{(m)} \sum_{b=0}^{m} \left\{ n_m(b) \tanh\left(\frac{(m-b)x_+ + bx_-}{m}\right) \frac{f(b)^\beta}{\sum_{b'=0}^{m} n_m(b') f(b')^\beta} \right\}, \tag{14}$$

$$x_- = \sum_{m=1}^{M} \lambda^{(m)} \sum_{b=0}^{m} \left\{ n_m(b) \tanh\left(\frac{(m-b)x_+ + bx_-}{m}\right) \frac{f(m-b)^\beta}{\sum_{b'=0}^{m} n_m(b') f(m-b')^\beta} \right\}, \tag{15}$$

where

$$n_m(b) = \binom{N_+}{m-b}\binom{N_-}{b} \tag{16}$$

counts the number of possible m-hyperedges containing $m-b$ agents with opinion x_+ and b agents with opinion x_-. These terms reflect the statistical weight of each group configuration in a polarized population. Moreover, the function

$$f(b) = \frac{\epsilon^{(m)}}{b(x_+ - x_-) + \epsilon^{(m)}} \tag{17}$$

defines the homophilic influence weight associated with a group where there are b agents with opinion x_-. The function decays as the internal disagreement in the group increases (i.e., as b grows), capturing the idea that agents are less influenced by dissimilar peers. Note that the small constant $\epsilon^{(m)}$ ensures regularization near zero opinion difference.

The polarized configuration given by Eqs. (14)–(15) is stable under perturbation of one of the agents if the following condition applies (see

$$1<\beta\sum_{m=1}^{M}\lambda^{(m)}\sum_{b=0}^{m}\left\{n_m(b)\tanh\left[\frac{(m-b)x_+ + bx_-}{m}\right]\frac{f(b)^{\beta}\left[\sum_{b'=0}^{m}n_m(b')f(b')^{\beta-1}g(b')\right]-f(b)^{\beta-1}g(b)\left[\sum_{b'=0}^{m}n_m(b')f(b')^{\beta}\right]}{\left[\sum_{b'=0}^{m}n_m(b')f(b')^{\beta}\right]^2}\right\}, \quad (18)$$

Supplementary Note 3 for the analytical derivation): where the function

$$g(b)=\frac{mb(x_+-x_-)+2b\epsilon^{(m)}}{\left[b(x_+-x_-)+\epsilon^{(m)}\right]^2} \quad (19)$$

appears in the derivative of the weighted influence term $f(b)$ and captures how sensitive the homophilic weight is to small perturbations in the agent's opinion. It depends on the opinion gap $x_+ - x_-$, the group composition b, and the small constant $\epsilon^{(m)}$ to avoid divergence.

The full stability condition in Eq. (18) ensures that small perturbations around the polarized configuration decay over time. Intuitively, it expresses a balance between the strength of homophilic influence (parametrized by β), the intensity of interactions $\lambda^{(m)}$, and the structure of group compositions. If this condition is violated, small perturbations grow and the polarized configuration becomes unstable.

Data availability

The numerical data used to generate the figures can be generated with the code provided in the manuscript. Moreover, these numerical data are also available from the authors upon request.

Code availability

The code needed to reproduce the results of the manuscript can be found in https://github.com/hperezmartinez/opinionHO.

Received: 16 July 2025; Accepted: 31 October 2025;
Published online: 17 November 2025

References

1. McElreath, R. & Boyd, R. *Mathematical Models of Social Evolution. A Guide for the Perplexed* (The University of Chicago Press, 2007).
2. Axelrod, R. *The Evolution of Cooperation* (Basic Books, 2006).
3. Castellano, C., Fortunato, S. & Loreto, V. Statistical physics of social dynamics. *Rev. Mod. Phys.* **81**, 591–646 (2009).
4. Jusup, M. et al. Social physics. *Phys. Rep.* **948**, 1–148 (2022).
5. Kubin, E. & Von Sikorski, C. The role of (social) media in political polarization: a systematic review. *Ann. Int. Commun. Assoc.* **45**, 188–206 (2021).
6. Cinelli, M. et al. The covid-19 social media infodemic. *Sci. Rep.* **10**, 16598 (2020).
7. Falkenberg, M. et al. Growing polarization around climate change on social media. *Nat. Clim. Change* **12**, 1114–1121 (2022).
8. Degroot, M. H. Reaching a Consensus. *J. Am. Stat. Assoc.* **69**, 118–121 (1974).
9. Deffuant, G., Neau, D., Amblard, F. & Weisbuch, G. Mixing beliefs among interacting agents. *Adv. Complex Syst.* **3**, 87–98 (2000).
10. Hegselmann, R. & Krause, U. Opinion dynamics and bounded confidence: models, analysis and simulation. *J. Artif. Soc. Soc. Simul.* **5**, 3 (2002).
11. Del Vicario, M., Scala, A., Caldarelli, G., Stanley, H. E. & Quattrociocchi, W. Modeling confirmation bias and polarization. *Sci. Rep.* **7**, 40391 (2017).
12. Giráldez-Cru, J., Zarco, C. & Cordón, O. Analyzing the extremization of opinions in a general framework of bounded confidence and repulsion. *Inf. Sci.* **609**, 1256–1270 (2022).
13. Leonard, N. E., Lipsitz, K., Bizyaeva, A., Franci, A. & Lelkes, Y. The nonlinear feedback dynamics of asymmetric political polarization. *Proc. Natl. Acad. Sci. USA* **118**, e2102149118 (2021).
14. Bizyaeva, A., Franci, A. & Leonard, N. E. Nonlinear opinion dynamics with tunable sensitivity. *IEEE Trans. Autom. Control* **68**, 1415–1430 (2023).
15. Galam, S. Unanimity, coexistence, and rigidity: three sides of polarization. *Entropy* **25**, 622 (2024).
16. Fiorina, M. P. & Abrams, S. J. Political polarization in the american public. *Annu. Rev. Polit. Sci.* **11**, 563–588 (2008).
17. American National Election Studies. ANES 2016 Time Series Study Full Release [dataset and documentation]. September 4, 2019 version. (2019).
18. Starnini, M. et al. Opinion dynamics: statistical physics and beyond. http://arxiv.org/abs/2507.11521 (2025).
19. Balietti, S., Getoor, L., Goldstein, D. G. & Watts, D. J. Reducing opinion polarization: effects of exposure to similar people with differing political views. *Proc. Natl. Acad. Sci. USA* **118**, e2112552118 (2021).
20. Wood, T. & Porter, E. The elusive backfire effect: mass attitudes' steadfast factual adherence. *Polit. Behav.* **41**, 135–163 (2019).
21. Isenberg, D. J. Group polarization: a critical review and meta-analysis. *J. Personal. Soc. Psychol.* **50**, 1141–1151 (1986).
22. Ziegler, R. & Sieber, J. 14: Group polarization. Res. Handbook Soc. Influence. https://www.elgaronline.com/edcollchap/book/9781035309672/chapter14.xml (2025).
23. Baumann, F., Lorenz-Spreen, P., Sokolov, I. M. & Starnini, M. Modeling echo chambers and polarization dynamics in social networks. *Phys. Rev. Lett.* **124**, 048301 (2020).
24. Santos, F. P., Lelkes, Y. & Levin, S. A. Link recommendation algorithms and dynamics of polarization in online social networks. *Proc. Natl. Acad. Sci. USA* **118**, e2102141118 (2021).
25. Pérez-Martínez, H., Mingueza, F. B., Soriano-Paños, D., Gómez-Gardeñes, J. & Floría, L. M. Polarized opinion states in static networks driven by limited information horizons. *Chaos Solit. Fractals* **175**, 113917 (2023).
26. Pedraza, L., Saintier, N., Pinasco, J. P., Balenzuela, P. & Anteneodo, C. Analytical insights from a model of opinion formation based on persuasive argument theory. *Phys. Rev. E* **112**, 014312 (2025).
27. Sunstein, C. R. The law of group polarization. *J. Polit. Philos.* **10**, 175–195 (2002).
28. Sunstein, C. R. Group polarization and 12 angry men. *Negotiat. J.* **23**, 443–447 (2007).
29. Holme, P. & Newman, M. E. J. Nonequilibrium phase transition in the coevolution of networks and opinions. *Phys. Rev. E* **74**, 056108 (2006).
30. Sood, V., Antal, T. & Redner, S. Voter models on heterogeneous networks. *Phys. Rev. E* **77**, 041121 (2008).
31. Vazquez, F., Eguíluz, V. M. & Miguel, M. S. Generic absorbing transition in coevolution dynamics. *Phys. Rev. Lett.* **100**, 108702 (2008).
32. Gómez-Gardeñes, J., Poncela, J., Mario Floría, L. & Moreno, Y. Natural selection of cooperation and degree hierarchy in heterogeneous populations. *J. Theor. Biol.* **253**, 296–301 (2008).
33. Klemm, K., Eguíluz, V. M., Toral, R. & San Miguel, M. Nonequilibrium transitions in complex networks: A model of social interaction. *Phys. Rev. E* **67**, 026120 (2003).
34. Guerra, B., Poncela, J., Gómez-Gardeñes, J., Latora, V. & Moreno, Y. Dynamical organization towards consensus in the axelrod model on complex networks. *Phys. Rev. E* **81**, 056105 (2010).
35. Santos, F. C., Pacheco, J. M. & Lenaerts, T. Evolutionary dynamics of social dilemmas in structured heterogeneous populations. *Proc. Natl. Acad. Sci. USA* **103**, 3490–3494 (2006).

36. Latora, V., Nicosia, V. & Russo, G. *Complex networks: principles, methods and applications* (Cambridge University Press, 2017).
37. Newman, M. *Networks* (Oxford university press, 2018).
38. Battiston, F. et al. Networks beyond pairwise interactions: structure and dynamics. *Phys. Rep.* **874**, 1–92 (2020).
39. Bick, C., Gross, E., Harrington, H. A. & Schaub, M. T. What are higher-order networks?. *SIAM Rev.* **65**, 686–731 (2023).
40. Majhi, S., Perc, M. & Ghosh, D. Dynamics on higher-order networks: A review. *J. R. Soc. Interface* **19**, 20220043 (2022).
41. Iacopini, I., Petri, G., Barrat, A. & Latora, V. Simplicial models of social contagion. *Nat. Commun.* **10**, 2485 (2019).
42. Lamata-Otín, S., Reyna-Lara, A. & Gómez-Gardeñes, J. Integrating virtual and physical interactions through higher-order networks to control epidemics. *Chaos Solit. Fractals* **189**, 115592 (2024).
43. Bretón-Fuertes, E. et al. Explosive adoption of corrupt behaviors in social systems with higher-order interactions. *Chaos Interdiscip. J. Nonlinear Sci.* **35**, 091103 (2025).
44. Sanders, G. S. & Baron, R. S. Is social comparison irrelevant for producing choice shifts?. *J. Exp. Soc. Psychol.* **13**, 303–314 (1977).
45. Burnstein, E. & Vinokur, A. Persuasive argumentation and social comparison as determinants of attitude polarization. *J. Exp. Soc. Psychol.* **13**, 315–332 (1977).
46. Hogg, M. A., Turner, J. C. & Davidson, B. Polarized norms and social frames of reference: a test of the self-categorization theory of group polarization. *Basic Appl. Soc. Psychol.* **11**, 77–100 (1990).
47. Neuhäuser, L., Mellor, A. & Lambiotte, R. Multibody interactions and nonlinear consensus dynamics on networked systems. *Phys. Rev. E* **101**, 032310 (2020).
48. Neuhäuser, L., Lambiotte, R. & Schaub, M. T. Consensus dynamics on temporal hypergraphs. *Phys. Rev. E* **104**, 064305 (2021).
49. Sahasrabuddhe, R., Neuhäuser, L. & Lambiotte, R. Modelling non-linear consensus dynamics on hypergraphs. *J. Phys. Complex.* **2**, 025006 (2021).
50. Galam, S. Spontaneous symmetry breaking, group decision-making, and beyond: 1. echo chambers and random polarization. *Symmetry* **16**, 1566 (2024).
51. Liuzza, D., Della Rossa, F., Lo Iudice, F. & De Lellis, P. Nonlinear Average Consensus Over Circulating Directed Hypergraphs. *IEEE Control Syst. Lett.* **9**, 1027–1032 (2025).
52. Liuzza, D., Rossa, F. D., Iudice, F. L. & Lellis, P. D. Synchronization and pinning control on circulating directed hypergraphs. *IEEE Transactions on Automatic Control* 1-16. https://ieeexplore.ieee.org/abstract/document/11123735 (2025).
53. Hickok, A., Kureh, Y., Brooks, H. Z., Feng, M. & Porter, M. A. A bounded-confidence model of opinion dynamics on hypergraphs. *SIAM J. Appl. Dyn. Syst.* **21**, 1–32 (2022).
54. Schawe, H. & Hernández, L. Higher order interactions destroy phase transitions in deffuant opinion dynamics model. *Commun. Phys.* **5**, 32 (2022).
55. Huang, C., Bian, H. & Han, W. Breaking the symmetry neutralizes the extremization under the repulsion and higher order interactions. *Chaos Solit. Fractals* **180**, 114544 (2024).
56. Lamata-Otín, S., Malizia, F., Latora, V., Frasca, M. & Gómez-Gardeñes, J. Hyperedge overlap drives synchronizability of systems with higher-order interactions. *Phys. Rev. E* **111**, 034302 (2025).
57. Malizia, F., Lamata-Otín, S., Frasca, M., Latora, V. & Gómez-Gardeñes, J. Hyperedge overlap drives explosive transitions in systems with higher-order interactions. *Nat. Commun.* **16**, 555 (2025).
58. Iacopini, I., Karsai, M. & Barrat, A. The temporal dynamics of group interactions in higher-order social networks. *Nat. Commun.* **15**, 7391 (2024).
59. Gallo, L., Lacasa, L., Latora, V. & Battiston, F. Higher-order correlations reveal complex memory in temporal hypergraphs. *Nat. Commun.* **15**, 4754 (2024).
60. Arregui-García, B., Longa, A., Lotito, Q. F., Meloni, S. & Cencetti, G. Patterns in temporal networks with higher-order egocentric structures. *Entropy* **26**, 256 (2024).

Acknowledgements

H.P.-M, S.L.-O, L.M.F., and J.G.-G. acknowledge financial support from the Departamento de Industria e Innovación del Gobierno de Aragón y Fondo Social Europeo (FENOL group grant E36-23R) and from Ministerio de Ciencia e Innovación (grants PID2020-113582GB-I00) and Ministerio de Ciencia, Innovación y Universidades (PID2023-147734NB-I00). H.P.-M and S.L.-O. acknowledge financial support from Gobierno de Aragón through a doctoral fellowship. D.S.-P. acknowledges financial support through grants JDC2022-048339-I and PID2021-128005NB- C21 funded by MCIN/AEI/10.13039/501100011033 and the European Union "NextGenerationEU/PRTR". F.M. acknowledges support from the Austrian Science Fund (FWF) through project 10.55776/PAT1652425.

Author contributions

All authors conceived the study and contributed to the design of the methodology. H.P.-M. performed the formal analysis and carried out the numerical simulations. S.L.-O. aided with numerical simulations and visualization. H.P.-M., S.L.-O., and F.M. wrote the original draft. L.M.F., J.G.-G., and D.S.-P. further contributed to review, editing, and approved the final version. D.S.-P. coordinated the research.

Competing interests

The authors declare no competing interests.

Additional information

Supplementary information The online version contains supplementary material available at https://doi.org/10.1038/s42005-025-02413-6.

Correspondence and requests for materials should be addressed to Jesús Gómez-Gardeñes or David Soriano-Paños.

Peer review information *Communications Physics* thanks the anonymous reviewers for their contribution to the peer review of this work. A peer review file is available.